

# Self-interference cancellation using dual-drive Mach-Zehnder modulator for in-band full-duplex radio-over-fiber system

Yunhao Zhang,<sup>1</sup> Shilin Xiao,<sup>1,\*</sup> Hanlin Feng,<sup>1</sup> Lu Zhang,<sup>1</sup> Zhao Zhou,<sup>2</sup>  
and Weisheng Hu<sup>1</sup>

<sup>1</sup>State Key Laboratory of Advanced Optical Communication System and Networks, Department of Electronic Engineering, Shanghai Jiao Tong University, Shanghai 200240, China

<sup>2</sup>State Grid Information & Communication Company of Hunan Electric Power Corp, Changsha 410000, China  
[\\*sxiao@sjtu.edu.cn](mailto:sxiao@sjtu.edu.cn)

**Abstract:** In this paper, we design a self-interference cancellation (SIC) scheme for in-band full-duplex (IBFD) radio-over-fiber (RoF) systems based on wavelength division multiplexing passive optical network (WDM-PON) architectures. By using a single dual-drive Mach-Zehnder modulator (DDMZM), over various bands up to 25 GHz, this proposed SIC system can simultaneously cancel the in-band downlink (DL) self-interference and modulate the recovered uplink (UL) radio frequency (RF) signal. OFDM-RF signals are used to study the cancellation performances of optical SIC system for the first time. Experimental results show more than 32-dB cancellation depth over 250-MHz bandwidth within 1-GHz RF band, as well as 300-MHz within 2.4-GHz and 400-MHz within 5-GHz band. As for 2.4-GHz RF band, 390.63-Mbps 16-QAM OFDM UL signal buried by strong in-band DL OFDM signal is well recovered. For broadband applications, more than 27-dB cancellation depth is achieved over 10 MHz~25 GHz wideband, so that up to 25 GHz RF band can be expanded for this IBFD WDM-RoF system.

©2015 Optical Society of America

OCIS codes: (060.4510) Optical communications; (350.4010) Microwaves.

---

## References and links

1. D. Wake, A. Nkansah, and N. J. Gomes, "Radio over fiber link design for next generation wireless systems," *J. Lightwave Technol.* **28**(16), 2456–2464 (2010).
2. Z. Cao, J. Yu, H. Zhou, W. Wang, M. Xia, J. Wang, and L. Chen, "WDM-RoF-PON architecture for flexible wireless and wire-line layout," *J. Opt. Commun. Netw.* **2**(2), 117–121 (2010).
3. A. T. Nguyen, Z. Cao, L. K. Efebvre, and L. Rusch, "Full-duplex WiFi analog transmission in RSOA-based radio-over-fiber system with wavelength-reuse," in *Proceedings of European Conference and Exhibition on Optical Communication (ECOC 2014)*, Paper P.7.21.
4. A. Sabharwal, P. Schniter, D. Guo, D. W. Bliss, S. Rangarajan, and R. Wichman, "In-band full-duplex wireless: challenges and opportunities," *IEEE J. Sel. Areas Comm.* **32**(9), 1637–1652 (2014).
5. B. Debaillie, B. van Liempd, B. Hershberg, J. Craninckx, K. Rikkinen, D. J. van den Broek, E. A. M. Klumperink, and B. Nauta, "In-band full-duplex transceiver technology for 5G mobile networks," in *Proceedings of IEEE European Solid-State Circuits Conference (ESSCIRC, 2015)*, 84–87.
6. P. A. Gamage, A. Nirmalathas, C. Lim, D. Novak, and R. Waterhouse, "Design and analysis of digitized RF-over-fiber links," *J. Lightwave Technol.* **27**(12), 2052–2061 (2009).
7. P. Dat, A. Kanno, N. Yamamoto, and T. Kawanishi, "Full-Duplex Transmission of LTE-A Carrier Aggregation Signal over a Bidirectional Seamless Fiber-Millimeter-Wave System," *J. Lightwave Technol.* (to be published).
8. H. Kim, J. H. Cho, S. Kim, K. U. Song, H. Lee, J. Lee, B. Kim, Y. Oh, J. Lee, and S. Hwang, "Radio-over-fiber system for TDD-based OFDMA wireless communication systems," *J. Lightwave Technol.* **25**(11), 3419–3427 (2007).
9. D. Wake, A. Nkansah, N. J. Gomes, G. De Valicourt, R. Brenot, M. Violas, Z. Liu, F. Ferreira, and S. Pato, "A comparison of radio over fiber link types for the support of wideband radio channels," *J. Lightwave Technol.* **28**(16), 2416–2422 (2010).

10. S. Gollakota and D. Katabi, "Zigzag decoding: combating hidden terminals in wireless networks", in *Proceedings of Annual International Conference on Mobile Computing and Networking (ACM, 2008)*, **38**(4), 159–170.
11. M. Jain, J. Choi, T. M. Kim, D. Bharadia, S. Seth, K. Srinivasan, P. Levis, S. Katti, and P. Sinha, "Practical, real-time, full duplex wireless," in *Proceedings of Annual International Conference on Mobile Computing and Networking (ACM, 2011)*, 301–312.
12. Q. Zhou, H. Feng, G. Scott, and M. P. Fok, "Wideband co-site interference cancellation based on hybrid electrical and optical techniques," *Opt. Lett.* **39**(22), 6537–6540 (2014).
13. J. Suarez, K. Kravtsov, and P. R. Prucnal, "Incoherent method of optical interference cancellation for radio-frequency communications," *IEEE J. Quantum Electron.* **45**(4), 402–408 (2009).
14. M. P. Chang, M. Fok, A. Hofmaier, and P. R. Prucnal, "Optical analog self-interference cancellation using electro-absorption modulators," *IEEE Microw. Wirel. Compon. Lett.* **23**(2), 99–101 (2013).
15. E. Ackerman, "Broad-band linearization of a Mach-Zehnder electrooptic modulator," *IEEE Trans. Microw. Theory Tech.* **47**(12), 2271–2279 (1999).
16. B. J. Kim and H. G. Ryu, "Self-Interference Cancellation using Mach-Zehnder Modulator for Full-Duplex Communication," in *Proceedings of IEEE International Conference on Information and Communication Technology Convergence (ICTC, 2014)*, 858–863.
17. J. Suarez, K. Kravtsov, and P. R. Prucnal, "Methods of feedback control for adaptive counter-phase optical interference cancellation," *IEEE Trans. Instrum. Meas.* **60**(2), 598–607 (2011).
18. 3GPP, 3GPP TS 36.104 version 11.9.0 Release 11, 2014.
19. M. Zhu, X. Liu, N. Chand, F. Effenberger, and G. K. Chang, "High-Capacity Mobile Fronthaul Supporting LTE-Advanced Carrier Aggregation and  $8 \times 8$  MIMO," in *Proceedings of Optical Fiber Communication Conference (OFC, 2015)*, M2J–3.

## 1. Introduction

Recently, radio-over-fiber (RoF) systems based on wavelength division multiplexing passive optical network (WDM-PON) architectures have been widely investigated for expanding coverage area and increasing overall capacity with a cost-efficient way [1–3]. Moreover, as for further RoF system, the in-band full-duplex (IBFD) transmission represents an attractive trend [4,5], which can simultaneously transmit and receive downlink (DL) and uplink (UL) radio frequency (RF) signals in the same frequency band between remote antenna units (RAUs) and user ends (UEs). Compared to frequently-used frequency-division duplex (FDD) and time-division duplex (TDD) mode [6–9], IBFD schemes significantly improve the throughput and extend the spectrum of system.

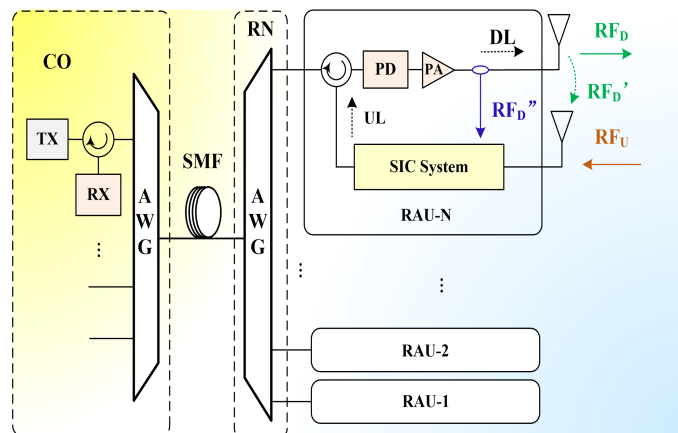


Fig. 1. Architecture of IBFD WDM-RoF system. Tx: transmitter; Rx: receiver; PD: photodetector; PA: power amplifier; SMF: single mode fiber; AWG: arrayed waveguide grating.

However, IBFD faces the challenges from the strong in-band self-interference (IBSI). Within the corresponding architecture as illustrated in Fig. 1, in each RAU, receive antenna gets to receive high-power IBSI from transmit antenna located nearby. This IBSI cannot be removed by preselected band-pass filter. In this case, self-interference cancellation (SIC)

systems are investigated in order to enable IBFD mode [4]. To remove IBSI in UL signal, the SIC system is installed following the receive antenna. The DL RF signal is duplicated as  $RF_D''$ , and then time and amplitude of the  $RF_D''$  and IBSI  $RF_D'$  are aligned in SIC system to subtract  $RF_D'$  and recover the desired UL signal  $RF_U$ . Due to bandwidth and linearity limitations of electrical devices, the electronic SIC schemes typically achieve about only 40-MHz cancellation bandwidth [10–12], which is not enough for the IBFD WDM-RoF systems. To overcome the limitation of cancellation bandwidth, optical or optical/electrical mixed schemes have been proposed [12–14]. An optical SIC scheme based on balanced photodetector (BPD) for signal subtraction were presented, in which two optical paths are needed before O/E conversion [14]. However, one RAU corresponds to only one output port of the arrayed waveguide grating (AWG) in remote node (RN), so that the employment of BPD in CO cannot be supported. Another optical/electrical mixed SIC scheme using Balun for signal inversion and electro-absorption modulators (EAMs) for modulation [12] reported 30-dB cancellation depth over 5.5-GHz bandwidth, which is limited by the operation bandwidth of Balun and EAMs. In IBFD WDM-RoF systems, broader wireless bandwidth is preferred for increasing system capacity.

In this paper, we propose and experimentally demonstrate a SIC system based on a dual-drive Mach-Zehnder Modulator (DDMZM) for IBFD WDM-RoF system. Due to alignment of  $RF_D''$  and  $RF_D'$  operated on electrical domain, only a single SMF is needed to equip, which is compatible for WDM-RoF system. OFDM-RF signals are used to study the cancellation performances of optical SIC systems for the first time. The corresponding experimental results show successful recovery of the self-interfered UL OFDM-RF signal in 2.4 GHz band, for the application of common-used wireless services. Moreover, the carrier frequency of this IBFD WDM-RoF system is expanded up to 25-GHz frequency band. To our knowledge this is the widest bandwidth with good cancellation depth of optical SIC system.

## 2. Architecture and principle

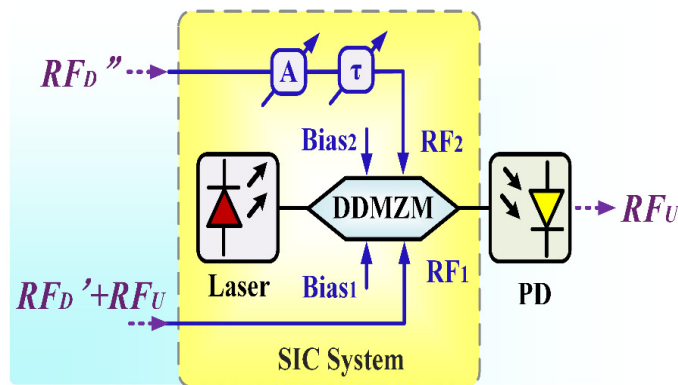


Fig. 2. The proposed SIC system.  $\tau$ : electrical time delay; A: electrical amplification.

The proposed SIC system is depicted in Fig. 2. The laser source provides UL seed light. The modules A and  $\tau$  on the upper path implement tunable electrical time delay and tunable electrical amplification of  $RF_D''$ , respectively.  $RF_D''$  is the replica of DL signal. In RAU, the signal received by receive antenna is the summary of DL self-interference  $RF_D'$  and UL signal of interest  $RF_U$ , marked as  $RF_D' + RF_U$ .

The principle of removing  $RF_D'$  in UL received signal is presented then.  $RF_D' + RF_U$  are delivered into  $RF_1$  port of DDMZM. Precisely-tuned amplified and delayed  $RF_D''$  are sent to  $RF_2$  port. Optical phase  $\phi_1$  and  $\phi_2$  of the bottom branch and upper branch are shown in Eq. (1) and Eq. (2), respectively.

$$\phi_1 = \frac{\pi}{V_\pi} V_1 = \frac{\pi}{V_\pi} (V_0 + V_\pi + RF_D' + RF_U). \quad (1)$$

$$\phi_2 = \frac{\pi}{V_\pi} V_2 = \frac{\pi}{V_\pi} (V_0 + \alpha RF_D''(\tau)). \quad (2)$$

$$\begin{aligned} E_{out} &= \frac{E_{in}}{2} (e^{j\phi_1} + e^{j\phi_2}) = E_{in} \cos \frac{\phi_1 - \phi_2}{2} e^{j \frac{\phi_1 + \phi_2}{2}} \\ &= E_{in} \cos \left( \frac{V_\pi}{2} + \frac{\pi}{2V_\pi} RF_U \right) e^{j \frac{\phi_1 + \phi_2}{2}}. \end{aligned} \quad (3)$$

$$P_{out} = P_{in} \cos^2 \left( \frac{V_\pi}{2} + \frac{\pi}{2V_\pi} RF_U \right). \quad (4)$$

$V_1$  and  $V_2$  represent the drive voltages, which are the summary of bias voltage and RF voltage on bottom branch and upper branch.  $V_0$  represents a random voltage in bias voltage range of DDMZM. We set  $V_{bias1}$  as  $V_0 + V_\pi$  and  $V_{bias2}$  as  $V_0$ , thus maintaining bias voltage difference of two arms  $V_\pi$ . Output optical field  $E_{out}$  and output optical power  $P_{out}$  are expressed in Eq. (3) and Eq. (4) [16], while  $E_{in}$  is input optical field and  $P_{in}$  is input optical power of DDMZM. By precisely-tuned amplified and delayed,  $RF_D''$  turns into  $\alpha RF_D''(\tau)$ , which is adjusted equal to  $RF_D'$ . So that shown by Eq. (3), the  $RF_D'$  is subtracted and  $RF_U$  is remained. The bias voltage  $V_{\pi/2}$  is the linear modulation bias point of MZM, set for the best E/O modulation of  $RF_U$  in Eq. (4). After optical power detection in PD, the UL signal of interest  $RF_U$  is well recovered. As mentioned above, the main step to realize SIC is tuning amplitude and time delay of  $RF_D''$ . In the practical mobile environments,  $RF_D'$  may vary with the change of wireless channel response. In this case, feed-back control like open-loop control or closed-loop control can be implemented for adaptive time delay and amplitude tuning [17].

### 3. Experiment setup and results

#### 3.1 SIC performance in common-used bands

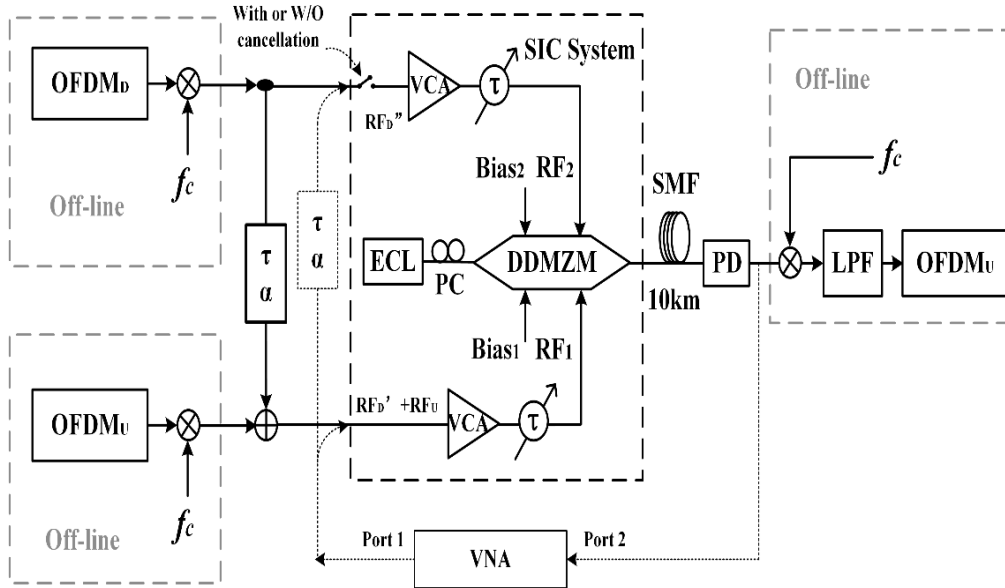


Fig. 3. Experimental setup. ECL: external cavity laser; PC: polarization controller; VCA: voltage-controlled amplifier;  $\tau$ : electrical time delay;  $\alpha$ : electrical attenuation; LPF: low-pass filter.

To experimentally prove the viability of this SIC system for IBFD systems, cancellation depth measurement and real-time in-band signal transmission are performed over several bands of interest. Experimental setup is configured according to Fig. 3. In SIC system, the functions of tunable electrical time delay and amplification are carried out by microwave voltage-controlled amplifiers (VCAs) and tunable microwave delay lines, respectively. To increase the flexibility of tuning, VCAs and delay lines are installed within both the up and bottom paths. The external cavity laser (ECL) is employed as laser source. The polarization controller (PC) is placed before DDMZM to control the polarization of input seed light. After 10-km SMF transmission, the desired UL signal is photo-detected in PD.

Cancellation depth over various frequency bands is measured firstly, the amount of which is determined by taking the difference between S21 curves of SIC system without and with cancellation. The 10-MHz~43.5-GHz vector network analyzer (VNA) (KEYSIGHT N5224A) is employed to measure the S21 response. As shown in Fig. 3, first the upper branch is disconnected, and voltage of bias1 and bias2 are set at linear modulation point to get S21 curve without cancellation. Then the upper branch is connected to VNA with random attenuation and delay of VNA's port 1 signal. In SIC system, the electrical amplification and delay are precisely tuned by the VCAs and tunable delay lines to obtain the S21 curve with the best cancellation.

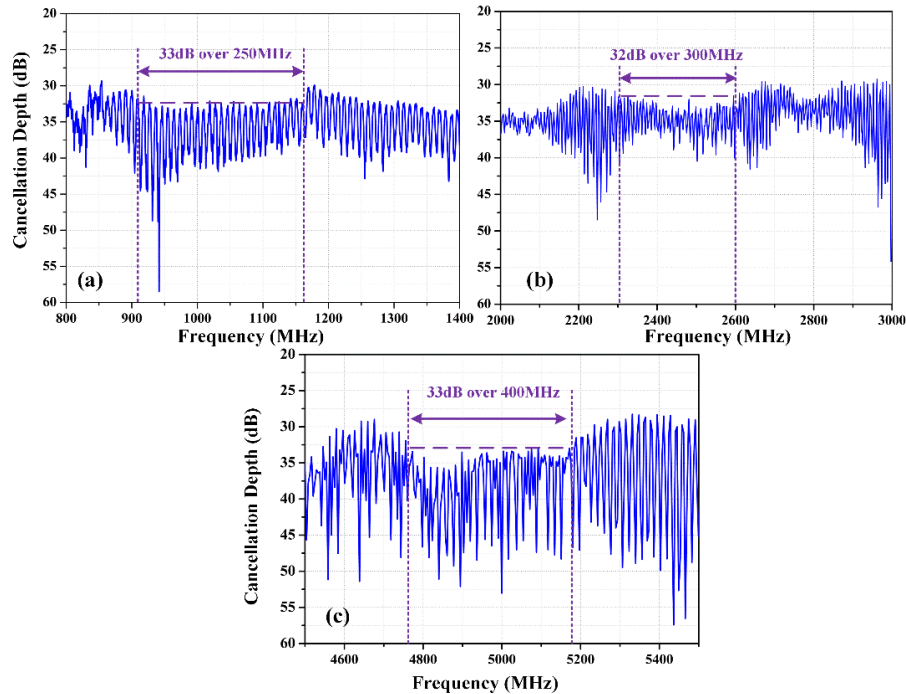


Fig. 4. Cancellation depth of SIC system at (a) 1.0-GHz, (b) 2.4-GHz and (c) 5.0-GHz band.

Common-used bands, for example, 1.0-GHz, 2.4-GHz and 5.0-GHz frequency bands are selected following the standard of wireless services like LTE, Wifi (IEEE 802.11), Bluetooth (IEEE 802.15) and WiMax (IEEE 802.16). Figures 4(a)-4(c) depict the cancellation depth in these frequency bands respectively. The results indicate the cancellation of more than 33 dB over 250-MHz bandwidth within 1.0-GHz band, more than 32 dB over 300-MHz bandwidth within 2.4-GHz and more than 33 dB over 400-MHz bandwidth within 5.0-GHz band. These properties enable SIC for multiple wireless services at various common-used frequency bands.

To perform real-time in-band signal transmission, the analog OFDM signals in 2.4-GHz RF band are selected to imitate Wifi-like UL and DL signals, since the analog OFDM-RF signal requires more linearity of SIC system than On-Off Keying (OOK) digital signal. VNA is now disconnected from the SIC system and offline OFDM-RF transmitters and a receiver are configured as shown in Fig. 3. The UL and DL OFDM signal are mixed with 2.4-GHz carrier frequency  $f_c$  respectively, both generated offline by an arbitrary waveform generator (AWG, Tektronix AWG7122C). After SIC and 10-km SMF transmission, desired UL signal is photo-detected, then sampled by a real-time oscilloscope (LeCroy SDA845Zi-A) and treated offline to observe the recovery of UL OFDM-RF signals. First we observe the cancellation on frequency domain. An RF spectrum analyzer (ROHDE&SCHWARZ FSUP, 20 Hz~50 GHz) is used for UL electrical spectrum measurement. The corresponding figure is depicted in Fig. 5, which indicates the electrical spectra of UL signal before and after cancellation, in which case UL desired signal occupies 19.53-MHz bandwidth while DL self-interference occupies 39.06-MHz bandwidth. Before cancellation, the  $RF_U$  is totally buried by the in-band self-interference  $RF_D'$ , and the spectrum is shown by the blue curve in Fig. 5. After cancellation, the signal power is reduced by 25 dB.  $RF_D'$  is removed and the  $RF_U$  is successfully recovered.

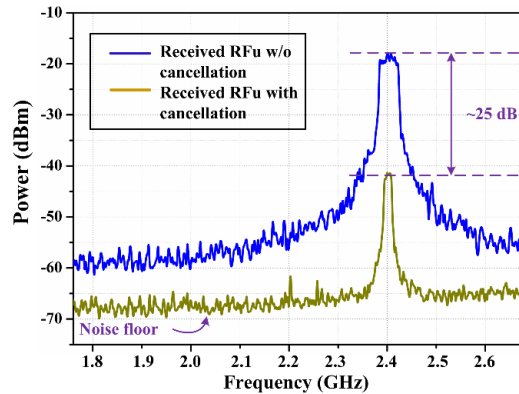


Fig. 5. Spectra of received  $RF_U$  without and with cancellation.

Then, the cancellation performance on time domain is observed with different data rates and different occupied bandwidths of OFDM signals. Corresponding to the case in Fig. 5, DL data rate is 156.25 Mbps and UL data rate is 78.12 Mbps. Figure 6(a) depicts the UL constellation diagram buried by  $RF_D'$ . After using our proposed scheme, the constellation diagram is well-recovered obviously, as shown in Fig. 6(d). The recovery of UL broadband OFDM signals proves that cancellation is not for instantaneous frequencies only, even though the sweep signal from port1 of VNA is single-tone frequency instantaneously when measuring cancellation depth. Moreover, UL and DL signals with higher bit rates and occupied bandwidths are investigated in this experiment in terms of constellation diagram, as depicted in Figs. 6(b)-6(c) and Figs. 6(e)-6(f). Constellation diagrams of the recovered UL OFDM-RF signals with 58.59 MHz and 97.66 MHz bandwidth are shown in Figs. 6(e)-6(f), respectively. To meet the performance requirements for the front-end of the base stations, we also measure the error vector magnitude (EVM) performances of recovered UL signals in these cases. The specified requirements of EVM in the 3GPP standard for 16-QAM is 12.5% [17]. The corresponding calculated EVMs of Figs. 6(d)-6(f) are 3.58%, 6.87% and 8.63% respectively, all under 12.5%. These experiment results demonstrate that the SIC system can support the recovery of at least 390.63-Mbps data rate of 16-QAM OFDM signal over 97.66-MHz within 2.4-GHz RF band, buried by in-band  $RF_D'$  with 117.19-MHz bandwidth, which would further confirm that at least ~100-MHz bandwidth in 2.4-GHz frequency band can be used for IBFD communication. These performances may be suitable for some of the next generation mobile standards such as carrier aggregation (CA), because one CA signal in LTE-A typically consists of five 20-MHz OFDM signals and occupies 100-MHz bandwidth in 2.4-GHz wireless band [18].

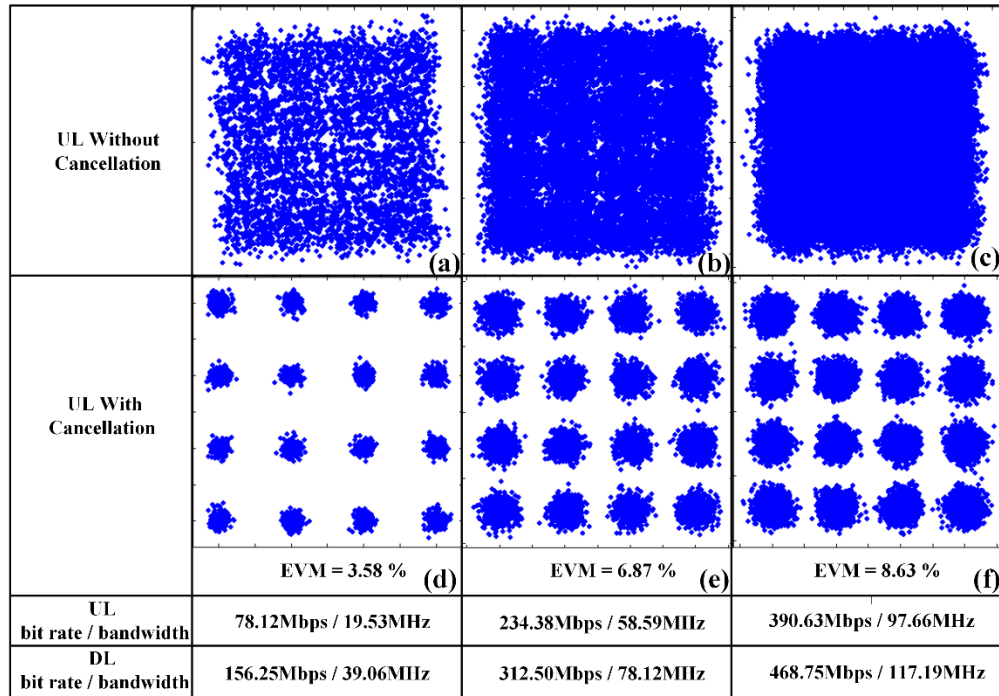


Fig. 6. Constellation diagrams of UL signals before (a-c) and after (d-e) cancellation.

### 3.2 Wideband SIC performance

Furthermore, we investigate the expansion of RF band for the WDM-RoF system. The cancellation depth in total 10MHz-25GHz frequency band is measured. As shown in Fig. 7, 27-dB total depth over 25-GHz bandwidth and 30-dB depth over about 9-GHz bandwidth is achieved. To our knowledge, this is the demonstration of widest cancellation bandwidth with good SIC performance.

In time domain, due to limitation of experiment condition, OFDM-RF SIC experiment at higher frequency band is not carried out. Instead, the high frequency and broadband performance is confirmed using 10-Gbps and 20-Gbps pseudo-random binary sequence (PRBS) signals. The offline UL OFDM-RF module in Fig. 3 is replaced by a pulse pattern generator (PPG, Agilent N4951B). The 10Gbps and 20Gbps PRBS signals are used as UL desired signal respectively, while the periodic strong sweeping signal from VNA between 10-MHz~25-GHz is used as in-band DL self-interference. The sweep time in one period is set 14.527 ms and sweep type is Linear Frequency. As interference signal, the number of points is set as 2001 to achieve enough frequency resolution. A sampling oscilloscope (Agilent 86103B) is employed as UL desired signal detector. Eye diagrams are observed to evaluate the wideband cancellation performance. Before cancellation, closed eyes caused by DL self-interference are shown in Figs. 8(a) and 8(c). After cancellation, the eyes are open, corresponding to 10-Gbps and 20-Gbps case in Figs. 8(b) and 8(d) respectively. Moreover, due to almost flat response from 10 MHz to 25 GHz broad RF bandwidth achieved, this bandwidth capability not only expands the RF band of IBFD WDM-RoF system to 25 GHz, but also enables simultaneous usage of multi-bandwidth services in total 10-MHz~25-GHz bands for RoF communication. The cancellation depth and bandwidth are mainly limited by the tuning precision of microwave VCA and microwave delay line.

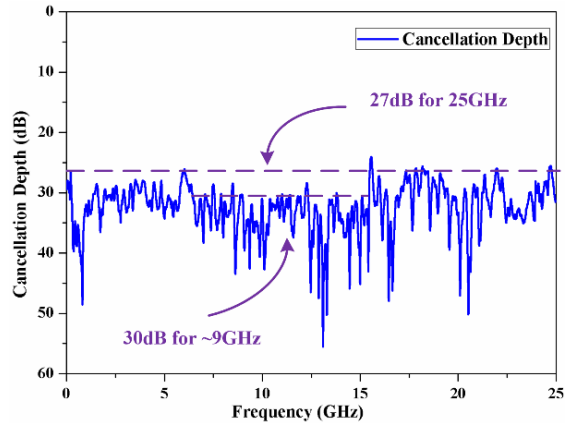


Fig. 7. Broadband cancellation depth.

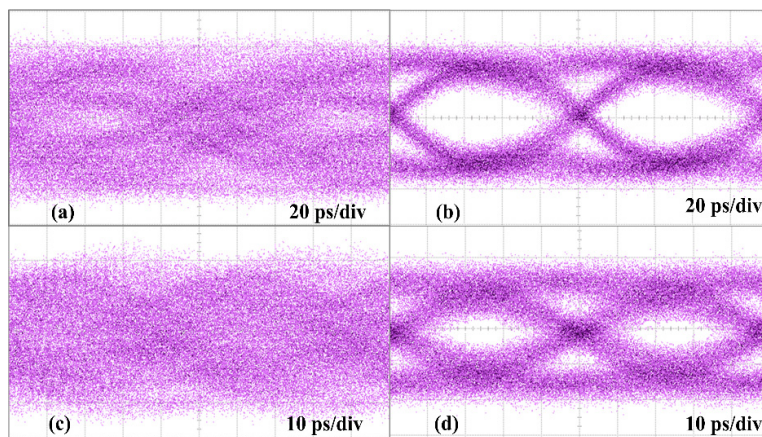


Fig. 8. Eye diagrams with data rate of 10 Gbps (a) before cancellation (b) after cancellation, and 20 Gbps (c) before cancellation (d) after cancellation.

#### 4. Conclusion

In this paper, we have experimentally demonstrated a SIC system for WDM-RoF system with IFBD mode. This SIC system based on DDMZM can cancel the DL interference with simultaneous modulation of UL RF signals. Cancellation performances in common-used bands for services like LTE, Wifi, Bluetooth and WiMax are experimentally studied, in which more than 32-dB cancellation depth over at least 240 MHz bandwidth are achieved. Successful recovery of UL 390.63-Mbps 16-QAM OFDM signal from DL 468.75-Mbps OFDM self-interference signal in 2.4-GHz RF band is obtained. For wideband application, more than 27-dB cancellation depth is achieved over total 10 MHz~25 GHz bandwidth. PRBS signals with 10-Gbps and 20-Gbps data rates are recovered from a wideband sweeping interference. The wideband SIC performance expands the RF band of this IBFD WDM-RoF system up to 25 GHz.

#### Acknowledgment

The work was jointly supported by the National Nature Science Fund of China (No.61271216, No. 61221001, No. 61090393 and No. 61433009), the National “973” Project of China (No. 2010CB328205, No. 2010CB328204 and No. 2012CB315602) and the National “863” Hi-tech Project of China (No. 2013AA013602 and No. 2012AA011301).